

NRL FR-7741

Empirical Bayes Estimation of the  
Probability Density of the Radar Cross  
Section of the Sea Surface

Maurice B. Owens

June 13, 1974

Naval Research Laboratory  
Washington D.C. 20362

REPORT DOCUMENTATION PAGE		READ INSTRUCTIONS BEFORE COMPLETING FORM
1. REPORT NUMBER NRL Report 7741	2. GOVT ACCESSION NO.	3. RECIPIENT'S CATALOG NUMBER
4. TITLE (and Subtitle) EMPIRICAL BAYES ESTIMATION OF THE PROBABILITY DENSITY OF THE RADAR CROSS SECTION OF THE SEA SURFACE		5. TYPE OF REPORT & PERIOD COVERED Interim
		6. PERFORMING ORG. REPORT NUMBER
7. AUTHOR(s) Maurice E. B. Owens		8. CONTRACT OR GRANT NUMBER(s)
9. PERFORMING ORGANIZATION NAME AND ADDRESS Naval Research Laboratory Washington, D.C. 20375		10. PROGRAM ELEMENT, PROJECT, TASK AREA & WORK UNIT NUMBERS NRL Problem R02-97 RR 021-01-41-5703
11. CONTROLLING OFFICE NAME AND ADDRESS Department of the Navy Office of Naval Research Arlington, Va. 22217		12. REPORT DATE June 13, 1974
		13. NUMBER OF PAGES 18
14. MONITORING AGENCY NAME & ADDRESS (if different from Controlling Office)		15. SECURITY CLASS. (of this report) Unclassified
		15a. DECLASSIFICATION/DOWNGRADING SCHEDULE
16. DISTRIBUTION STATEMENT (of this Report) Approved for public release; distribution unlimited.		
17. DISTRIBUTION STATEMENT (of the abstract entered in Block 20, if different from Report)		
18. SUPPLEMENTARY NOTES		
19. KEY WORDS (Continue on reverse side if necessary and identify by block number) Sea clutter                      Density estimation Composite surface              Clutter simulation		
20. ABSTRACT (Continue on reverse side if necessary and identify by block number)  When sea clutter is viewed at low grazing angles with a high-resolution radar, the envelope of the return does not have a Rayleigh distribution. Based on the concept of the composite sea surface scattering model, the probability density of the return can be written as the integral of the product of two factors. The first factor is the probability density function of the radar cross section (RCS) of the illuminated patch, and the second is the density of  (Continued)		

DD FORM 1473  
1 JAN 73EDITION OF 1 NOV 65 IS OBSOLETE  
S/N 0102-014-6601

i

SECURITY CLASSIFICATION OF THIS PAGE (When Data Entered)

## 20. Abstract (Continued)

the return conditioned on the cross section. If the patch is large, one can assume that the cross section remains constant. But for a small patch it varies randomly. Two sets of nonparametric estimates of the RCS density of a small patch were obtained. One group of estimates is based on experimental data and the other on a simulation consisting of theoretical models. Because the estimation procedures differ for the two groups, no statistical comparison was made; however, the two sets are considered in good agreement.

## CONTENTS

INTRODUCTION .....	1
THE RCS OF A PATCH OF THE SEA SURFACE .....	2
NONPARAMETRIC ESTIMATION OF A PROBABILITY DENSITY .....	3
THE DATA .....	5
DATA ANALYSIS .....	5
SIMULATION .....	7
NUMERICAL RESULTS .....	9
SUMMARY AND CONCLUSIONS .....	12
ACKNOWLEDGMENT .....	12
REFERENCES .....	13

\_\_\_\_\_

\_\_\_\_\_

## EMPIRICAL BAYES ESTIMATION OF THE PROBABILITY DENSITY OF THE RADAR CROSS SECTION OF THE SEA SURFACE

### INTRODUCTION

It has been recognized for some time that when sea clutter is viewed at low grazing angles with a high-resolution radar the envelope of the return is not distributed according to a Rayleigh distribution; see Nathanson [1] and Skolnik [2]. A number of researchers have attempted to characterize the distribution of the return as a function of various experimental parameters. For example, Nathanson [1] uses the coefficient of variation (ratio of standard deviation to mean) as a measure of departure from a Rayleigh distribution, and Trunk and George [3] modeled the distribution of the return with both log-normal and contaminated-normal distributions, Ballard [4] being one of the first to suggest the log-normal distribution. The recent works by Guinard [5], Valenzuela, Laing and Daley [6], and Wright [7] are concerned with predicting the expected value of the return. Although some of these alternative models are good approximations to experimental results, they yield little insight into the physical mechanism to which the true distribution of the envelope of the return can be attributed.

In a more recent paper, Trunk [8] considered a composite scattering model to explain the non-Rayleigh nature of sea clutter when viewed at low grazing angles with a high-resolution radar. Hereinafter the term *high-resolution* radar refers to a radar which illuminates a patch of sea that is not large relative to the wave structure of that sea. The rationale behind this composite model is that the radar cross section (RCS) of the illuminated patch is a function of the slope of that patch. This function is extremely sensitive to the grazing angle whenever the grazing angle is less than the critical angle, a nominal value of the critical angle being  $10^\circ$ . Thus, the variation of the RCS of the patch depends on the variation of the slope of the patch. Since the slope does not vary in a deterministic fashion, the sea surface can be considered to be a fluctuating target. In this report nonparametric estimates of probability density functions of the RCS of the sea surface, obtained from both real data and computer simulations, are presented.

Valenzuela and Laing have taken a similar approach in Ref. 9. Assuming a perfectly conducting sea and assuming that the slope of the surface is normally distributed, they obtain theoretical probability densities for the RCS of the patch. Because these densities depend only on the grazing angle and the root-mean-square (rms) of the slope of the patch, they do not reflect the orientation of the radar relative to the surface waves. This is an important consideration in the high-resolution case [10].

## THE RCS OF A PATCH OF THE SEA SURFACE

Consider a particular patch of sea surface  $\mathcal{P}$  at a fixed point in time. At this instant the apparent RCS of the patch is given by

$$\sigma = \int \int_{(x,y) \in \mathcal{P}} \sigma(\alpha) g(x,y,z) dx dy \quad (1)$$

where

$z$  is the height of the surface at the point  $(x,y)$

$\alpha = \alpha(x,y,z)$  is the angle between the normal to the surface at  $(x,y,z)$  and the vector from the point to the radar antenna

$\sigma(\alpha)$  is the reflected power given the incident angle  $\alpha$  (to be detailed later)

$g(x,y,z)$  is the two-way antenna power gain at the point  $(x,y,z)$ .

Now as time passes or as the patch moves along the surface,  $\sigma$  will vary in a stochastic manner. Thus in general the RCS of a patch of the sea surface is a random variable, denoted  $\underline{\sigma}$ , with probability density  $f_1(\sigma)$ .

As a consequence of the composite model,\* the probability density of the return is given by

$$p(r) = \int_0^{\infty} p_1(r|\sigma) f_1(\sigma) d\sigma,$$

where  $p_1(r|\sigma)$  is the conditional density of the return given  $\sigma$ . Most of the work in the study of returns from sea clutter has been concerned with the various properties of  $p(r)$ . However, from an analysis based on data taken with frequency-agile, high-resolution radar, Trunk [8] concluded that the form of  $f_1$  has an important influence on that of  $p$ . These data, used in this report, consist of independent, paired samples (two pulses at different frequencies) of the return, the time between the paired samples being small. Under the assumption that  $p_1(r|\sigma)$  is essentially of the form

$$p_1(r|\sigma) = \frac{1}{\sigma} h\left(\frac{r}{\sigma}\right),$$

Trunk noticed that the ratio of the two samples in a given patch will change very little during the time interval corresponding to the time between the paired observations. On the basis of these ratios, Trunk was able to make inferences concerning the nature of  $p_1(r|\sigma)$ . He concluded that  $p_1(r|\sigma)$  depends on polarization and direction relative to the wave fronts.

In this report, nonparametric estimators of the density  $f_1(\sigma)$ , or equivalently the probability density of  $10 \log_{10} \underline{\sigma}$ , are developed. Estimates of the density are computed for experimental data as well as for data generated by a computer model.

\*The composite sea-surface scattering mode is based on the hypothesis that the only contribution of the large wave structure in the determination of  $\sigma$  is in the tilting of the slightly rough surface composed of capillary waves.

## NONPARAMETRIC ESTIMATION OF A PROBABILITY DENSITY

Let  $x_1, \dots, x_N$  be a sequence of identically distributed random variables, each having probability density  $f$ . An estimator of  $f$  evaluated at the point  $y$  of the form

$$\hat{f}_N(y) = \frac{1}{N} \sum_{i=1}^N K_N(y, x_i)$$

for a known function  $K_N$  is called a kernel estimator. A common form of the function  $K_N$  is

$$K_N(y, x) = \frac{1}{h_1(N)} K_1[(y-x)/h_1(N)]$$

for some function  $K_1$  and sequence of numbers  $h_1(N)$ . It is generally assumed that  $K_1$  is even, continuous, and non-negative and that

$$\int_{-\infty}^{\infty} K_1(x) dx = 1.$$

Under these two conditions, the estimator  $\hat{f}_N$  is a density function. If  $K_1$  satisfies the above conditions and if

$$\sup_{-\infty < x < \infty} |K_1(x)| < \infty$$

and

$$\lim_{|x| \rightarrow \infty} |xK_1(x)| = 0,$$

then it is shown in Ref. 11 that  $\hat{f}_N(y)$  is asymptotically consistent in  $N$  when  $f$  is continuous and when

$$\lim_{N \rightarrow \infty} Nh_1(N) = \infty$$

and

$$\lim_{N \rightarrow \infty} h_1(N) = 0.$$

However, Rosenblatt [12] shows that under fairly general and reasonable conditions there is no estimator, say  $\hat{f}_N(y)$ , of  $f(y)$  for which

$$E\hat{f}_N(y) = f(y)$$

for all  $y$ . If the reader is interested in the area of nonparametric density estimation, he is referred to the two basic papers by Rosenblatt [12] and by Parzen [11] and to a recent survey article by Wegman [13].

Before one can apply a kernel estimator to estimate a probability density, he must specify a function  $K_1$  and a number  $h_1(N)$ . Exactly how one should proceed in making this choice appears to be an open question. In any case, the function

$$K_1(x) = \frac{1}{\pi} \left( \frac{\sin x}{x} \right)^2$$

has been employed with some success. Another common choice of the kernel is the standardized Gaussian density, but the former will be used in this analysis. The sequence of constants employed here is given by

$$h_1(N) = \frac{20}{\sqrt{N}}$$

in decibels. Thus, if  $f$  is the density function of  $\underline{x} = 10 \log_{10} \underline{\sigma}$  then

$$\hat{f}_N(y) = \frac{1}{20\sqrt{N}\pi} \sum_{i=1}^N \left[ \frac{\sin t_i}{t_i} \right]^2 \quad (2)$$

is an estimator of  $f(y)$  where

$$t_i = (y - \underline{x}_i) \sqrt{N}/20$$

and  $\underline{x}_1, \dots, \underline{x}_N$  are independently distributed according to the density  $f$ .

Recall that the probability density of the return is

$$p(r) = \int_0^{\infty} p_1(r|\sigma) f_1(\sigma) d\sigma,$$

and the density to be estimated is  $f(x)$ , where  $\underline{x} = 10 \log_{10} \underline{\sigma}$ .

The difficulty in applying Eq. (2) to obtain an estimate  $f(x)$  based on experimental data is that the random variable  $\underline{x}$  is not observed directly. The data consists of samples of the random variable  $\underline{r}$ . If the conditional density  $p_1(r|\sigma)$  is known precisely, there are a number of procedures, called empirical Bayes methods (see Ref. 14 and references therein), that could be employed to estimate  $f_1(\sigma)$  or equivalently  $f(x)$ . But, as it was previously mentioned, Trunk [8] has shown that  $p_1(r|\sigma)$  depends on various experimental conditions. Moreover, it is safe to assume that

$$p_1(r|\sigma) = \frac{1}{\sigma} h\left(\frac{r}{\sigma}\right)$$

for some density  $h$ . Now let

$$a = \int_0^{\infty} rh(r)dr,$$

and hence, note that for all  $\sigma$

$$E[r|\sigma] = a\sigma.$$

In this situation a procedure, based on the concepts in Refs. 15 and 16, can be employed to use Eq. (2) as an estimator of  $f(x)$ . Consider the following sampling scheme. For each  $i = 1, \dots, N$  select a sample, say  $\sigma_i$ , from the distribution having density  $f_1$  and then select  $k$  samples, denoted  $r_{i1}, \dots, r_{ik}$  from the distribution having density  $p_1(r|\sigma_i)$ . Observe that

$$E(r_{ij}) = a\sigma_i$$

for  $j = 1, \dots, k$  and that

$$a\hat{\sigma}_i = \frac{1}{k} \sum_{j=1}^k r_{ij} \quad (3)$$

is an estimator of  $a\sigma_i$ . Now

$$\underline{x}_i = 10 \log_{10} a\hat{\sigma}_i = 10 \log_{10} \hat{\sigma}_i + 10 \log_{10} a. \quad (4)$$

That is  $\underline{x}_i$  is an estimate of  $10 \log_{10} \sigma_i$  shifted by a constant which is independent of  $i$ . As  $k$  increases without bound,  $\underline{x}_i$  converges to  $10 \log_{10} \sigma_i$  in probability. Thus, the  $\underline{x}_i$  defined by Eq. (4) can be used in Eq. (2) to obtain an estimate of  $f(y)$ .

## THE DATA

The data, on which the analysis in this report is based, were taken by an airborne, high-resolution, noncoherent, pulsed, X-band radar, the radar being capable of frequency diversity on a pulse-to-pulse basis. The PRF was 2560 Hz, and adjacent pulses were transmitted at different frequencies. Data were taken with both horizontal and vertical polarizations. The pulse length was 20-ns, the grazing angle  $4.7^\circ$ , the range 2 n.mi., yielding an illuminated patch of approximately 10 ft in range and 105 ft in azimuth. Upwind, downwind, and crosswind measurements were made. The experiment was performed on March 11 and 12, 1969, when the aircraft flew 200 miles off the east coast of Virginia. During the time of the experiment, 8-ft waves, 12-ft swells, and 25- to 31-knot winds were observed.

## DATA ANALYSIS

Procedures for obtaining a nonparametric estimate of a probability density function have been detailed in a previous section; however, these procedures cannot be applied to these data in a routine manner to estimate accurately the probability density of the

Table 1  
Decorrelation Times and Sampling Intervals\*

Direction	Polarization	Decorrelation Time (ms)	Sampling Interval (ms)	No. Samples in Interval	No. Intervals
Upwind	Horizontal	106	33	12	256
Upwind	Vertical	193	63	22	256
Downwind	Horizontal	131	39	14	208
Downwind	Vertical	168	51	18	256
Crosswind	Horizontal	112	33	12	256
Crosswind	Vertical	31	9	4	192

\*From G. V. Trunk, IEEE Trans. AES-9, No. 1, 110 (Jan. 1973), Table IV.

normalized RCS. The problem here is that the RCS of the illuminated patch is constantly changing, but the RCS can be considered to remain constant over a small time interval. Trunk calculated the correlation functions for data records taken over a 12.8-s time interval and presented the decorrelation times in Table VI in Ref. 8, the decorrelation time being that time which the correlation function is equal to  $1/e$ . Selected decorrelation times taken from Trunk's Table VI are presented in Table 1.

Since the samples of the return from sea clutter taken at least 10 ms apart can be considered uncorrelated when the RCS of the patch remains constant (see Ref. 3), it is felt that the decorrelation times listed in Table 1 are good estimates of the times required for the RCS of the illuminated patch to decorrelate. Based on these times a time interval, called the sampling interval, was selected during which it is assumed that the RCS of the patch essentially remains constant. The lengths of these time intervals, each of which is approximately a third of the corresponding decorrelation time, are listed in the fourth column of Table 1. Averages of the data points falling within the same sampling interval can be used in Eq. (2) to estimate the RCS of the patch that the radar was viewing during that time.

For each record every eighth sample was selected to form a new record with samples spaced 3 ms apart. Since adjacent samples in the new records were recorded at different frequencies, adjacent observations can be assumed to be uncorrelated, and samples recorded at the same frequency are spaced 6 ms apart. The total numbers of samples in the sampling intervals are listed in the fifth column of Table 1, and the total numbers of intervals employed in this analysis are given in the sixth column.

The procedure for computing an estimate of the probability density for each of the six data sets indicated in Table 1 is as follows:

1. Using Eq. (3) average the returns in each sampling interval.

2. Compute the estimates  $\underline{x}_i$  of the RCS in dB of the patch corresponding to the  $i$ th sampling interval by Eq. (4).
3. Estimate the probability density of the return using Eq. (2).

The results of this analysis are presented in another section of this report.

*Remark:* Note that the procedure for obtaining estimates of the RCS corresponding to the sampling intervals is a simple average. However, the manner in which the sampling intervals were selected, together with the composite model, gives a basis for interpretation of the results. This will become apparent when the results of the data analysis are compared with those obtained from a computer simulation.

### SIMULATION

The RCS of a given patch of sea surface is given by Eq. (1), and the evaluation of that integral is straightforward once values of the function  $\sigma(\alpha)$  is available. For horizontal polarization the RCS [10] is given by\*

$$\sigma_{HH} = 4\pi k^4 \cos^4 \alpha \left| \frac{(\epsilon - 1)}{[\cos \alpha + (\epsilon - \sin^2 \alpha)^{1/2}]^2} \right|^2 W(2k \sin \alpha) \quad (5)$$

and for vertical

$$\sigma_{VV} = 4\pi k^4 \cos^4 \alpha \left| \frac{(\epsilon - 1)[\epsilon + (\epsilon - 1) \sin^2 \alpha]}{[\epsilon \cos \alpha + (\epsilon - \sin^2 \alpha)^{1/2}]^2} \right|^2 W(2k \sin \alpha), \quad (6)$$

where

$\epsilon$  is the complex dielectric constant

$k = 2\pi/\lambda$

$KW(K)dK = S(\omega)d\omega$ ,

$\omega^2 = K^2g$ , where  $g$  is the acceleration of gravity

$K = 2k \sin \alpha$

$S(\omega)$  is the power density spectrum of the sea surface.

Thus, the problem of calculating  $\sigma(\alpha)$  has been reduced to that of calculating  $\alpha$ .

Recall that  $\alpha = \alpha(x, y, z)$  is the angle between the vector from the point  $(x, y, z)$  to the radar and the normal to the sea surface at the point  $(x, y, z)$ . The latter is defined as that vector which is normal to the large wave structure at the point  $(x, y, z)$ .

---

\*The notation  $\sigma_{HH}$  refers to the power of the return when the signal is transmitted and received with horizontal polarization.

Here the approach taken to calculate  $\alpha$  is similar to that employed in Ref. 8 and is based on a concept of constructing a realization of the sea surface given by Neumann and Pierson [17]. A solution of the Lagrangian equations of motion for a fully developed sea surface is expressed parametrically in  $\delta$  and  $y$ :

$$\begin{aligned} x &= \delta - \sum_{i=1}^N a_i \sin \left[ \frac{\omega_i^2}{g} (\delta \cos \theta_i + y \sin \theta_i) + \gamma_i \right], \\ y &= y \\ z &= \sum_{i=1}^N a_i \cos \left[ \frac{\omega_i^2}{g} (\delta \cos \theta_i + y \sin \theta_i) + \gamma_i \right], \end{aligned} \tag{7}$$

where  $\gamma_i$  are independent uniformly distributed phases between 0 and  $2\pi$ , and  $\theta_i$  are independent Gaussian random variables with zero mean and standard deviation of  $10^\circ$ . The increasing frequencies  $\omega_1, \dots, \omega_N$  are given by

$$\omega_i = \begin{cases} (\omega'_{i-1} + \omega'_i)/2, & i = 1, \dots, (N-1) \\ \omega'_{N-1}, & i = N \end{cases}$$

where  $\omega'_0 = 0$ ,  $\omega'_N = \infty$ , and for  $i = 1, \dots, N$

$$\int_{\omega'_{i-1}}^{\omega'_i} S(\omega) d\omega \Big/ \int_0^\infty S(\omega) d\omega = 1/N.$$

The coefficients in  $a_i$  in Eq. (7) are independent Gaussian random variables with zero mean and variance

$$\sigma_{a_i}^2 = 2 \int_{\omega'_{i-1}}^{\omega'_i} S(\omega) d\omega \approx 2S(\omega_i)(\omega'_i - \omega'_{i-1}).$$

It should be mentioned that temporal variation in Eq. (7) can be introduced by replacing the random phase  $\gamma_i$  by  $(\gamma_i + \omega_i t)$ .

For this study  $N = 100$  and

$$S(\omega) = \frac{dg^2}{\omega^5} \exp[-b(g/u\omega)^4],$$

which is the Kitaigorodskii spectrum [18,19], where  $d = 0.0081$ ,  $b = 0.74$ , and  $u$  is the windspeed.

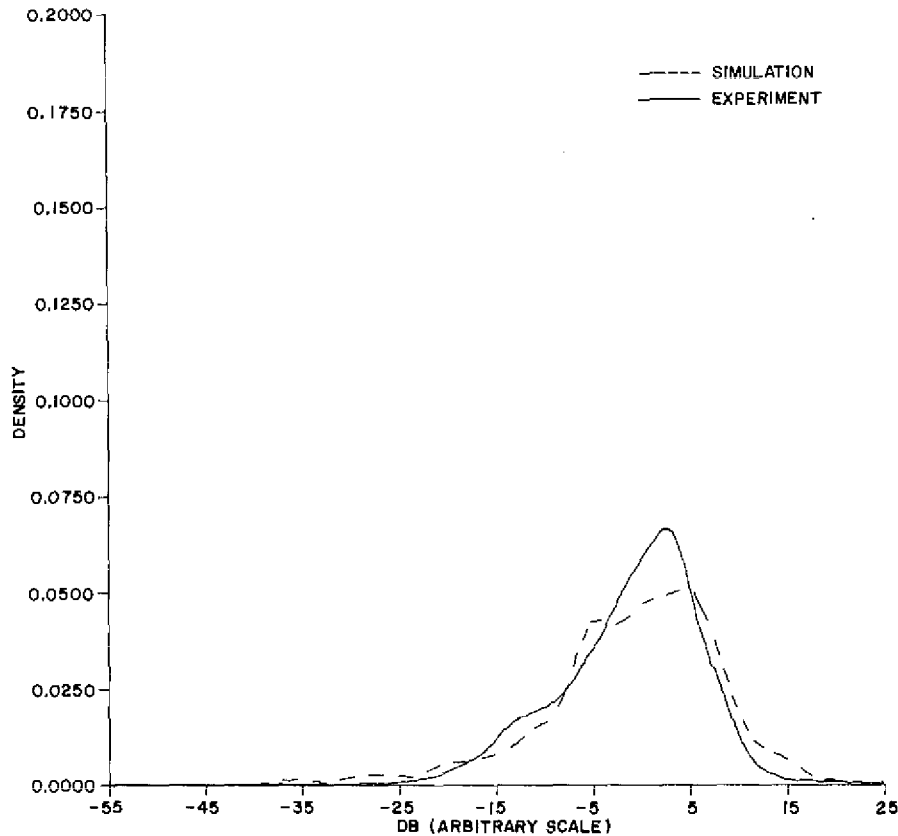


Fig. 1--Estimated probability densities of normalized RCS;  
horizontal polarization, upwind

To construct a series of realizations of the sea surface, first determine the values of  $\omega_i$  and  $\sigma_{a_i}^2$ . Then for each realization, select the values of  $a_i$ ,  $\theta_i$ , and  $\gamma_i$  from their respective distributions. The value of  $\sigma$  for each realization can be calculated using Eq. (1), (5), and (6). Once a series of values of  $\sigma$  is available, the probability density function of  $10 \log \underline{g}$  can be estimated through Eq. (2).

## NUMERICAL RESULTS

The nonparametric estimates of the probability densities of  $10 \log \underline{g}$  for the six experimental situations of Table 1 are displayed in Figs. 1-6. In each figure estimated density depicted by the solid line is based on the experimental data and that represented by the dashed line is based on 200 simulated observations of  $\underline{g}$ .

Before the densities were estimated, each set of simulated observations was shifted so that the median of the simulated observations coincided with the median of the corresponding set of experimental observations. Since simulated upwind and downwind

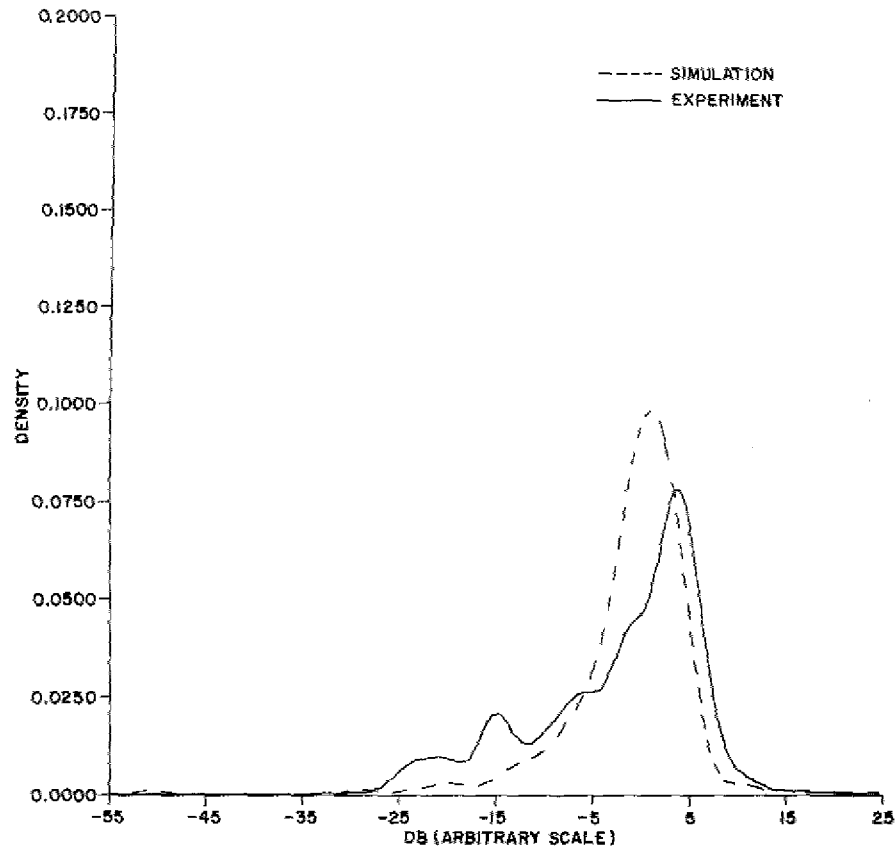


Fig. 2—Estimated probability densities of normalized RCS; vertical polarization, upwind

measurements are the same, the estimated density in Fig. 1 is the same as that in Fig. 3. The same applies to Figs. 2 and 4. Since the simulation is a model of a fully developed sea, the wind speed used was 18 knots corresponding to the observed 8-ft waves [8] as opposed to the reported 25- to 31-knot wind.

In comparing the experimentally derived results with those based on the simulation, one should remember that the observations of  $\log \underline{\sigma}$  are obtained through different mechanisms in the two cases. In the simulation the only errors associated with observations of  $\log \underline{\sigma}$  are caused by the inaccuracies of the model and the mathematical calculations therein. Whereas, in the experiment  $\log \underline{\sigma}$  is observed with an error having essentially two components. The first component of error arises from the fact that on a given sample the only observable variable is the return  $\underline{r}$ ,  $\underline{r}$  being related to  $\underline{\sigma}$  through the density  $p_1(r|\sigma)$ . This component of error is further complicated in that various properties of  $p_1(r|\sigma)$ , which is not known explicitly, depend on experimental parameters. To reduce this component of error, a number of observed values of  $\underline{r}$  are averaged to obtain an estimate of  $\underline{\sigma}$ , the average being carried out under the assumption that  $\underline{\sigma}$  remains constant over the appropriate time interval. Of course, this assumption is not precisely correct, thus introducing a second component of error in the estimate of  $\underline{\sigma}$ .

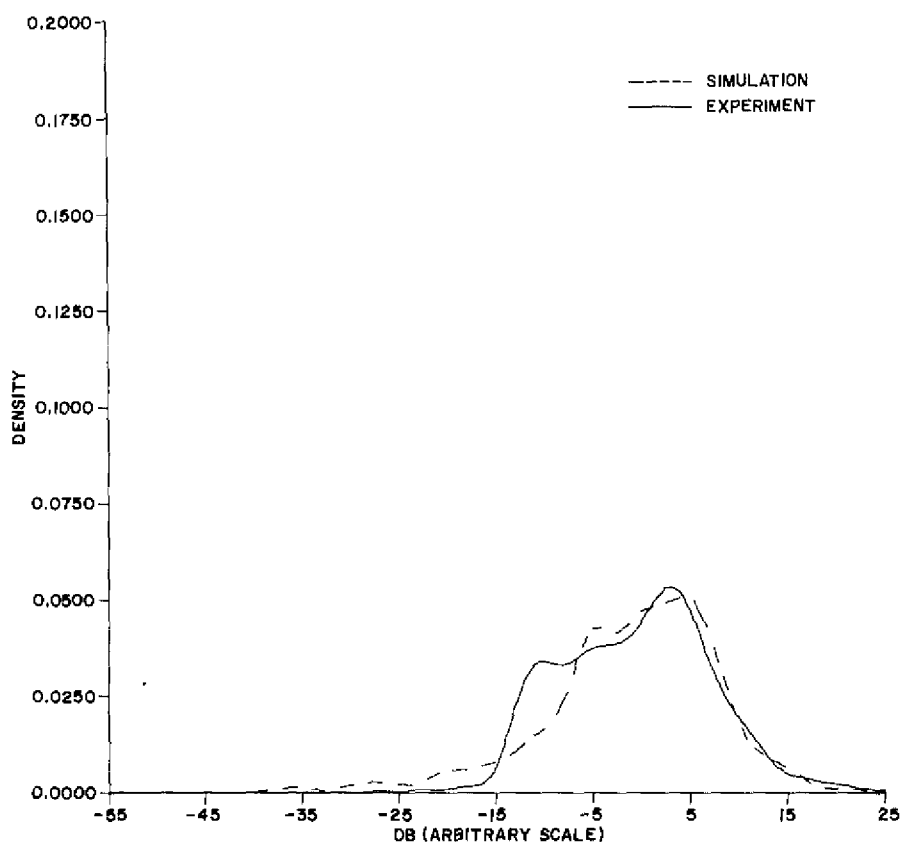


Fig. 3—Estimated probability densities of normalized RCS;  
horizontal polarization, downwind

Each pair of densities as displayed in Figs. 1-6 could be subjected to a hypothetical test that the two members of each pair arose from a common parent population. This analysis has not been performed, since in each case the hypothesis would be rejected. However, considering the complexity of the mechanism producing sea clutter at low grazing angles and that the two sets of results are not based on the same set of observables, the author feels that the agreement is good. The greatest discrepancy between the simulated and experimentally derived results is found in Fig. 6. This is attributed to the relatively small decorrelation time as indicated in Table 1 for this case. That is, the RCS of the patch is changing rapidly, and thus its value estimated by averaging only from observations (see Table 1) is subject to large error. This explains the fact that in Fig. 6 the variance of the estimated density based on the experiment is larger than that of the density based on the simulation.

Note the irregularity of the densities corresponding to upwind and downwind measurements. It is conjectured that this effect is caused by shadowing of the patch by the large wave structure. Moreover, the densities for vertical polarization are more peaked than those for horizontal polarization. This supports the conclusion in Ref. 8 that the density of the return (i.e.  $p(r)$ ) is closer to a Rayleigh distribution for vertical polarization than for horizontal polarization.

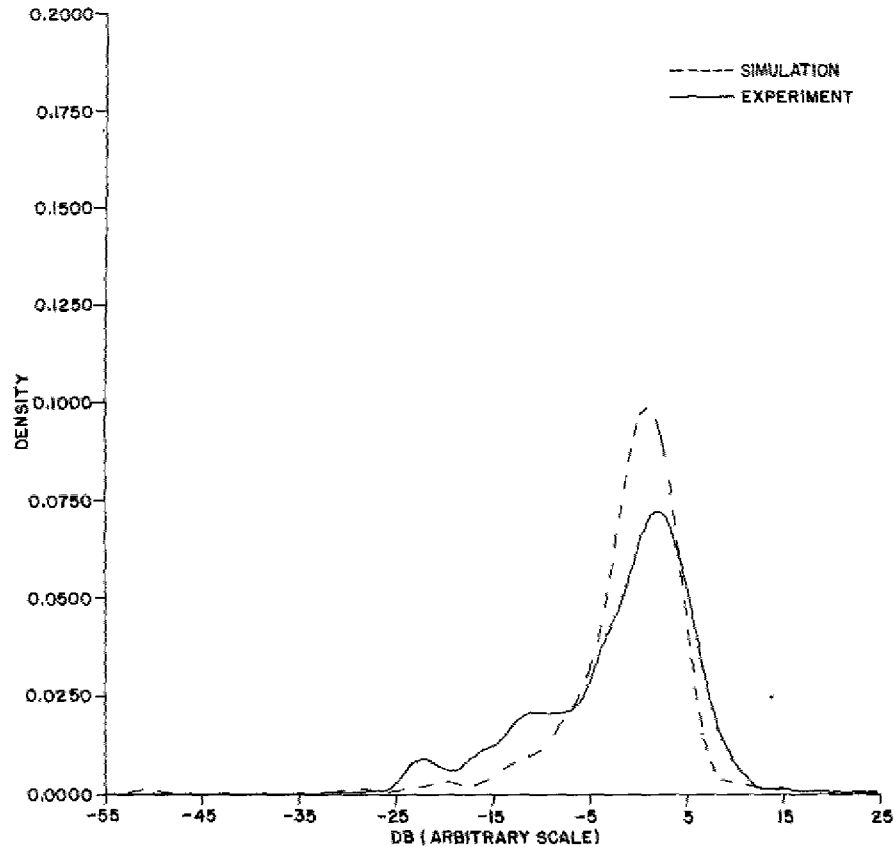


Fig. 4—Estimated probability densities of normalized RCS;  
vertical polarization, downwind

#### SUMMARY AND CONCLUSIONS

Two methods for estimating the first-order probability density function of the apparent RCS of a patch of the sea surface have been presented. One procedure is applicable to experimental data, whereas the other is based on a computer simulation. In the opinion of the author, results obtained from the two methods are in good agreement, and thus, the computer simulation can be employed to predict the first-order statistical variation of the RCS of a patch of sea surface. Moreover, it is possible that an extension of the simulation described in this report could be employed to examine temporal statistical properties of the RCS of a small patch of sea surface.

#### ACKNOWLEDGMENTS

The author wishes to thank Dr. G. V. Trunk for his helpful discussions and suggestions and Mr. J. C. Daley for bringing the results in Ref. 9 to his attention.

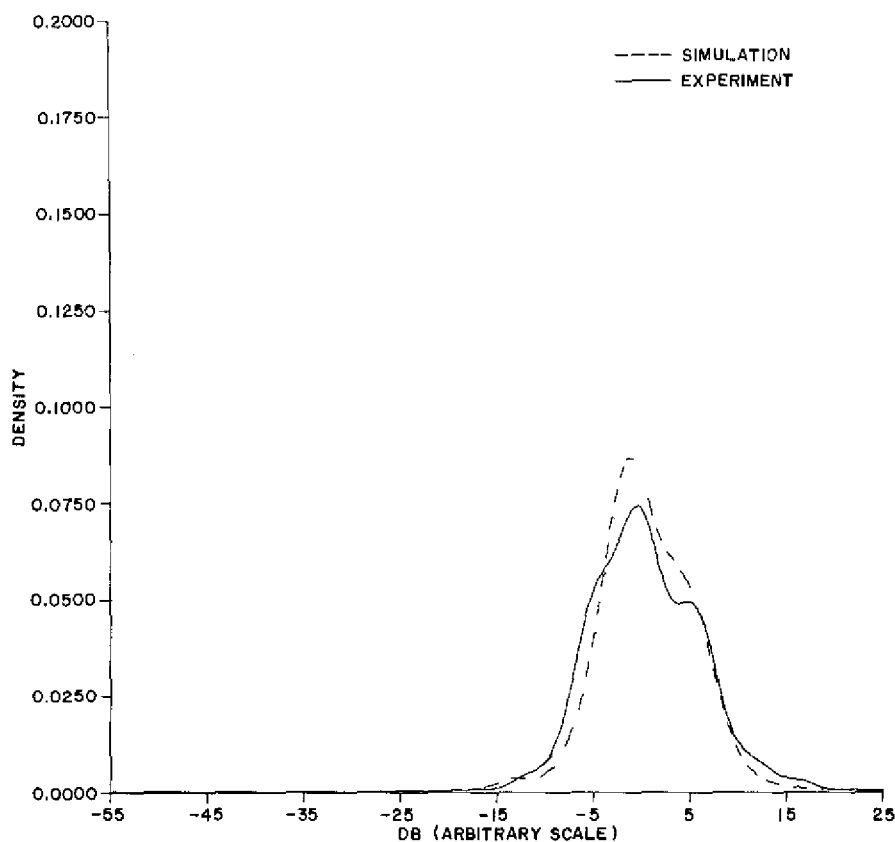


Fig. 5—Estimated probability densities of normalized RCS;  
horizontal polarization, crosswind

## REFERENCES

1. F.E. Nathanson, *Radar Design Principles*, McGraw-Hill Book Co., New York, 1969.
2. M.I. Skolnik, "A Review of Radar Sea Echo." NRL Memorandum Report 2025, July 1969.
3. G.V. Trunk and S.F. George, "Detection of Targets in Non-Gaussian Sea Clutter," *IEEE Trans.*, AES-6, No. 5, 620-628 (1970).
4. A.H. Ballard, "Detection of Radar Signals in Log-normal Sea Clutter," TRW Systems Document 7425-8509-TO-000, May 31, 1966.
5. N.W. Guinard and J.C. Daley, "An Experimental Study of a Sea Clutter Model," *Proc. IEEE*, 58, No. 4, 543-550 (Apr. 1970).
6. G.R. Valenzuela, M.B. Laing, and J.C. Daley, "Ocean Spectra for the High-Frequency Waves as Determined From Airborne Radar Measurements," *J. Marine Res.*, 29, No. 2, 69-84 (1971).

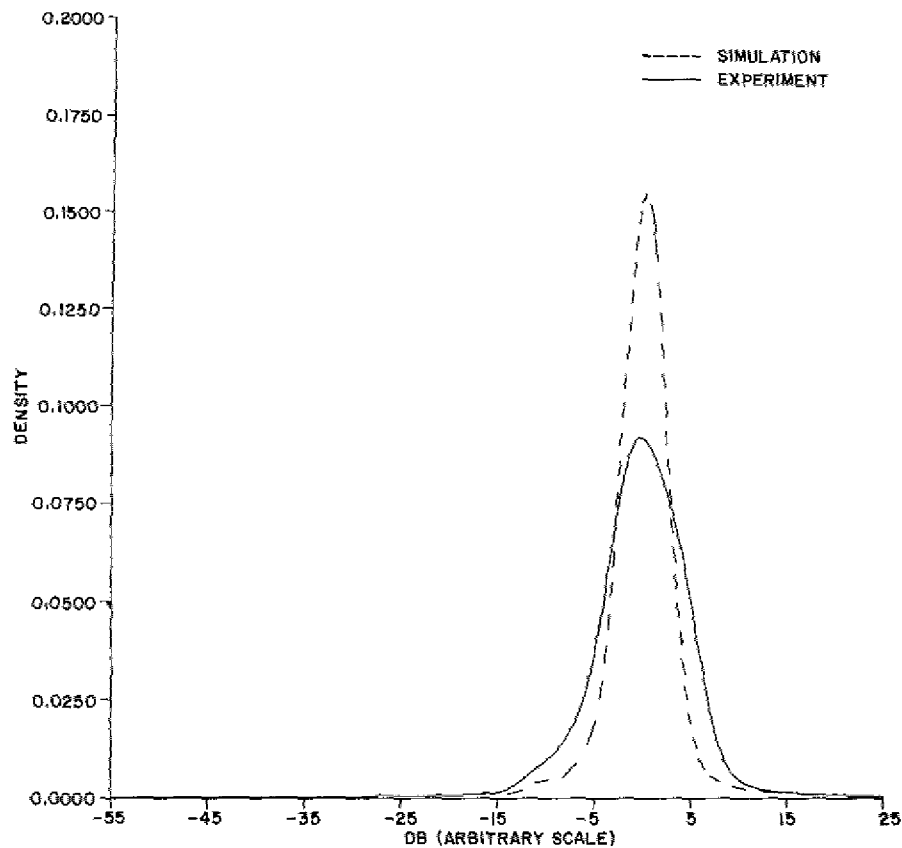


Fig. 6—Estimated probability densities of normalized RCS;  
vertical polarization, crosswind

7. J.W. Wright, "A New Model for Sea Clutter," *IEEE Trans.*, AP-16, No. 2, 217-223 (Mar. 1968).
8. G.V. Trunk, "Radar Properties of Non-Rayleigh Sea Clutter," *IEEE Trans.*, AES-8, No. 2, 196-204 (Mar. 1972).
9. G.R. Valenzuela and M.B. Laing, "On the Statistics of Sea Clutter," NRL Report 7349, Dec. 1971.
10. G.V. Trunk, "Modification of Radar Properties of Non-Rayleigh Sea Clutter," *IEEE Trans.*, AES-9, No. 1, 110 (Jan. 1973).
11. E. Parzen, "On the Estimation of a Probability Density Function and the Mode," *Ann. Math. Stat.*, 33, 1065-1076 (1962).
12. M. Rosenblatt, "Remarks on Some Nonparametric Estimates of a Density Function," *Ann. Math. Stat.*, 27, 832-837 (1956).

13. E.J. Wegman, "Nonparametric Probability Density Estimation: I. A Summary of Available Methods," *Technometrics*, 14, No. 3, 533-546 (Aug. 1972).
14. J.S. Maritz, *Empirical Bayes Estimation*, Methuen and Co. Ltd., London, 1970.
15. G.K. Bennett and H.F. Martz, "A Continuously Smooth Empirical Bayes Estimator," *Proceedings of the Symposium on Empirical Bayes Estimation and Computing in Statistics*, T.A. Atchison and H.F. Martz, editors, Texas Tech University, Lubboch, Texas, August 1969, pp. 93-109.
16. J.R. Rutherford and R.G. Krutchkoff, "The Empirical Bayes Approach: Estimating the Prior Distribution," *Biometrika*, 54, 326-328 (1967).
17. G. Neumann and W.J. Pierson, Jr., *Principles of Physical Oceanography*, Prentice-Hall, Englewood Cliffs, N.J., 1966.
18. S.A. Kitaigorodskii, "Application of the Theory of Similarity to the Analysis of Wind Generated Wave Motion as a Stochastic Process," *Izv. Akad. Nauk SSSR, Ser. Geofiz.*, 1, 105-117; English translation in Vol. 1, 73-80 (1961).
19. W.J. Pierson, Jr. and L. Moskowitz, "A Proposed Spectral Form for Fully Developed Wind Seas Based on the Similarity Theory of S.A. Kitaigorodskii," *J. Geophys. Res.*, 69, No. 24, 5181-5190 (Dec. 1964).